

# Behavior of plaster with water-repellent additive under natural aging

S. D. S. Rodrigues<sup>1\*</sup>, M. A. Silva<sup>2</sup>, J. G. G. Sousa<sup>3</sup>, N. C. Olivier<sup>1</sup>

<sup>1</sup>Universidade Federal do Vale do São Francisco, Graduate Program in Materials Science, Av. Antônio C. Magalhães 510, Juazeiro, BA, Brazil

<sup>2</sup>Universidade Federal do Vale do São Francisco, Computer Engineering Department, Juazeiro, BA, Brazil

<sup>3</sup>Universidade Federal do Vale do São Francisco, Department of Civil Engineering, Juazeiro, BA, Brazil

## Abstract

This research evaluates the behavior of plaster with a water-repellent additive when submitted to a natural aging process. Casting plaster and silane/siloxane-based water-repellent were used as materials. The water/plaster ratio was set at 0.7 and the contents of 0.2% and 0.4% of water-repellent were used, in relation to the plaster mass. Plaster pastes without water-repellent (reference) and containing mass water-repellent were evaluated at 'zero' age and after 30, 60, 90, 120, and 150 days of natural aging. After 150 days of natural aging, it was observed that the mechanical properties of the material (compressive strength and hardness) did not undergo significant variations and remained above the minimum required by a standard. The addition of water-repellent resulted in a considerable reduction in water absorption, demonstrating the water repellency capacity of the material, compared to the reference specimen.

**Keywords:** calcium sulfate hemihydrate, silane, siloxane, water-repellent, weathering.

## INTRODUCTION

Plaster, a calcium sulfate hemihydrate ( $\text{CaSO}_4 \cdot 1/2\text{H}_2\text{O}$ ) is an aerial binder, obtained from the calcination of the mineral gypsum. The use of surface plaster in civil construction has become increasingly intense due to the ease of finishing, molding, and thermal and acoustic insulation behavior [1]. In addition, the Gesseiro pole, in the Araripe region, in Pernambuco state (Brazil), also uses this material in the production of blocks and slabs. Gypsum is an interesting alternative from an environmental aspect due to its low energy demand when compared to other inorganic materials, such as Portland cement and lime. This occurs because of the low temperature required for the calcination of the gypsum mineral, to obtain calcium sulfate hemihydrate. However, the material dissolves when in permanent contact with water, which makes it difficult to use in wet places. Therefore, it is important to develop technologies that allow the use of this material in these environments.

The use of water-repellent additives has been investigated, as a way to minimize the effects of moisture on plaster performance. The hydrofuge of plaster blocks can occur directly when the additive is mixed with water during the production of the block or after manufacturing when used as a paint [2]. Although the use of water-repellents has become a common practice to provide greater durability to plaster specimens, issues such as the durability of the water-repellent action have not yet been clarified. Hence, it was decided to study the durability of this material through

the aging process. The concept of aging is understood as the set of physical and chemical changes that occur in the structure of the material and have an impact on performance and durability. The aging of construction materials mainly concerns construction elements exposed to climatic factors, such as high and low temperature, solar radiation, and rainfall, causing degradation phenomena. Resistance to these factors is essential during the period of use [3].

With regard to natural aging, long-term methodologies can be used. These techniques aim to analyze the behavior of materials or components when subjected to real exposure conditions, observing true degradation rates, instead of accelerated degradation rates in the laboratory [4]. Current research assesses durability through natural aging in cement and hydraulic lime-based coatings for example [3, 5]. As for plaster, its use is often limited to research involving composite materials, where it is evaluated in association with other materials [6, 7]. Regarding the addition of water-repellents and the verification of their waterproofing capacity, the evaluation of long-term durability has still been underexplored [8]. The analysis through natural aging contributes to the development of technologies that provide resistance to the weather, in addition to implying the estimation of the durability of the material [3] and, consequently, of the constructive element. In that regard, this research aims to evaluate the properties of beta casting plaster used for the production of vertical sealing elements, with the addition of mass water-repellent, when exposed to the weather through natural aging. The material was evaluated for hardness, axial compressive strength, water absorption by total immersion, and water absorption by capillary action, in addition to morphological and chemical analysis using scanning electron microscopy (SEM) and dot

\*sheila-dsr@hotmail.com

https://orcid.org/0000-0002-0902-1794

mapping by energy dispersive spectroscopy (EDS).

## MATERIALS AND METHODS

**Materials. Beta plaster:** a casting beta plaster (calcium sulfate hemihydrate) obtained at the Gesseiro do Araripe Pole, in Araripina-PE, Brazil, was used. The plaster used was characterized for particle size, bulk density and free and crystallization water content [9, 10]. For the determination of particle size, 210 g of the oven-dried sample at  $40\pm 4$  °C was used, from which a sample of  $50\pm 1$  g was taken by quartering and passed through a sieve with an opening of 0.29 mm. The sieving was considered finished when, between two weighings, the mass passing through the sieves was less than 0.1 g. The procedure was performed twice, and the result was calculated by the average of the masses, which did not differ from the latter by 5%. The passing percentage R was determined by:

$$R = \frac{m}{M} \cdot 100 \quad (\text{A})$$

in which m is the passing material (g) and M is the initial mass (g). For the determination of bulk density, the method consists of passing the plaster sample through a funnel, until filling a container of known volume (cylindrical container, made of non-corrosive material, with a capacity of 1000 cm<sup>3</sup>). After filling the container, the surface of the container was scraped and the plaster was weighed. The bulk density, B<sub>d</sub> (kg/m<sup>3</sup>), was calculated by:

$$B_d = \frac{M}{V} \quad (\text{B})$$

in which M is the plaster mass of the container (g), and V is the volume of the container (cm<sup>3</sup>). The average value between two determinations was considered, as long as the difference between them was less than 5% of the average value. The determination of free water was carried out by verifying the mass loss of 50 g of plaster in an oven at  $40\pm 4$  °C. The crystallization water was measured by the mass loss of 2 g of plaster at  $230\pm 10$  °C. In addition, X-ray diffraction (XRD) analysis was performed to identify the phases present in the sample. Measurements were taken in a powder diffractometer (Miniflex, Rigaku) with CuK $\alpha$  radiation ( $\lambda=1.5418$  Å) operating at 40 kV and 15 mA in the continuous mode with steps of 0.02°, speed of 10 °/min, in a 10° to 90° range and room temperature. The sample's experimental diffractogram was compared with the theoretical patterns available in the PDF2 (Powder Diffraction File) crystallographic database from the Bragg crystalline peak positions and intensities and the most like references using a software (X'Pert HighScore Plus, PANalytical). Fourier transform infrared spectroscopy (FTIR) was performed on calcium sulfate dihydrate for the identification of their functional groups. Measurements were taken with a spectrometer (IRTracer-100, Shimadzu) in the region between 4000 and 400 cm<sup>-1</sup> with 45 scans and a resolution of 4 cm<sup>-1</sup>.

**Water repellent of mass:** a mass water-repellent was used for plaster waterproofing. The determination of the specific mass was carried out following a normative procedure [11]. Because the water-repellent was a liquid, the standard prescribes the use of a pycnometer. The test consisted of weighing the empty pycnometer and then filling it with water and immersing it in a thermoregulatory bath until reaching  $25\pm 1$  °C for 30 min. After the thermoregulatory bath, the pycnometer was superficially dried and weighed. Subsequently, the pycnometer was filled with the water repellent sample and after the thermoregulatory bath, its weight was recorded. The specific mass of the water repellent was determined by:

$$d_l = \frac{m_c - m_a}{m_b - m_a} \quad (\text{C})$$

in which, d<sub>l</sub> is the liquid additive density at 25 °C, m<sub>a</sub> is the empty pycnometer mass (g), m<sub>b</sub> is the pycnometer mass plus water mass (g), and m<sub>c</sub> is the pycnometer mass plus sample mass (g). In addition, an analysis by FTIR was performed to identify the characteristic functional groups of the polymer components, from the absorption of each type of chemical bond, using the same test specifications applied for the plaster.

**Definition of dosages:** reference pastes without water-repellent (GR), and pastes with mass water-repellent additive (GR2/GR4) were produced, using distilled water and admitting a water/plaster ratio of 0.7, in order to maintain the same proportion used in the commercial manufacture of plaster blocks at the Gesseiro do Araripe Pole [12]. Regarding the water-repellent, the proportions evaluated were 2 and 4 mL/kg, defined according to the plaster mass used, adopted based on the manufacturer's recommendation. The identification of mixtures and the dosage of water-repellent are described in Table I. The reference plaster paste was prepared by sprinkling gypsum powder over water for 1 min [13]. Then, the material was left to rest for 2 min and, after this time, it was mixed for 1 min/s in a circular motion. The paste was then transferred to a mold, taking care to eliminate air bubbles, remaining for 2 h until demolding. After demolding, the specimens remained in an oven at  $40\pm 5$  °C to dry, which took place for 4 days. The procedure for the production of plaster paste with the mass water-repellent additive followed the same description above, adding it to the kneading water in the proportion indicated in Table I.

**Methods. Natural aging:** the specimens were exposed to the weather for the natural aging process, from January

Table I - Identification of the mixtures used.

Mixture	Constituent	MWR (mL/kg of plaster)
GR	Reference	0
GH2	MWR	2
GH4	MWR	4

MWR: mass water-repellent.

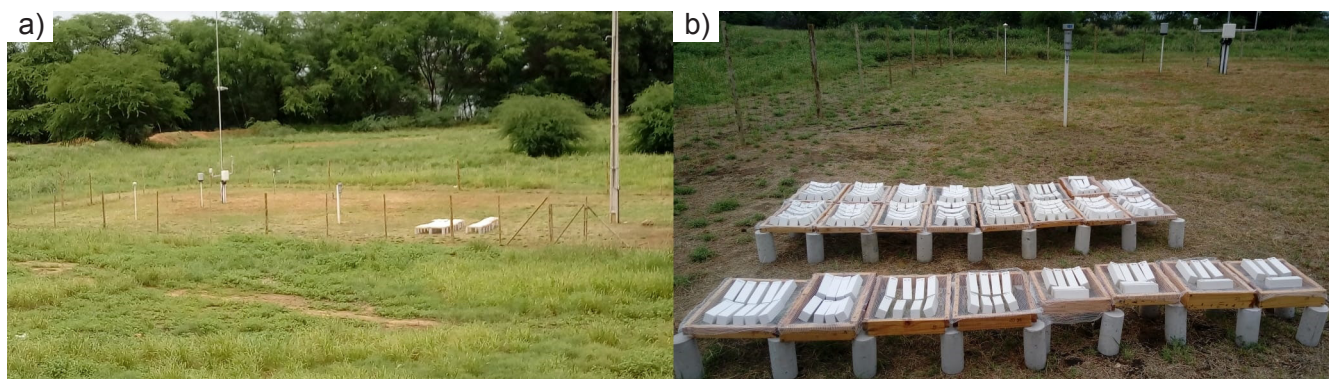


Figure 1: Images showing the location of the Univasf Automatic Meteorological Station, where the specimens were placed.

Table II - Meteorological data referring to months of exposure to natural aging (data from the Univasf Meteorology Laboratory website).

Weather data	Natural aging period				
	30 days Jan-Feb	60 days Feb-Mar	90 days Mar-Apr	120 days Apr-May	150 days May-Jun
Reference evapotranspiration (ET <sub>o</sub> mm/day)	144.4	153.1	129.1	124.4	103.3
Precipitation (mm)	69.6	28.2	98.0	21.4	9.8
Global radiation (MJ.m <sup>-2</sup> .day <sup>-1</sup> )	21.5	23.2	20.4	18.8	16.5
Average minimum air temperature (°C)	23.3	23.5	23.1	22.5	21.4
Average maximum air temperature (°C)	33.2	33.0	32.5	31.9	30.8
Average air temperature (°C)	27.8	27.7	27.1	26.5	25.4
Minimum relative humidity (%)	40.5	35.8	42.4	42.3	42.5
Maximum relative humidity (%)	80.9	80.3	85.0	84.7	84.1
Maximum wind speed at 10 m (m/s)	7.3	7.3	7.1	7.7	7.8

to June 2020. Thus, they were taken to the Automatic Meteorological Station, located at Universidade Federal do Vale do São Francisco (Univasf), Campus Juazeiro-BA, Brazil (latitude 9°24'37"S, longitude 40°30'50"W), for monitoring meteorological information, where they were displayed on screens to allow rainwater to flow. The specimens exposed to environmental climatic conditions are shown in Fig. 1. Table II shows a summary of meteorological data over the period in which the specimens remained in the field. Monthly averages were calculated using spreadsheets available on the Univasf Meteorology Laboratory website (Labmet) as a basis. The values in Table II are related to the exposure periods (30, 60, 90, 120, and 150 days), thus, from the moment they were placed in the field, until the first 30 days of exposure, 69.6 mm of precipitation occurred. In the next 30 days, precipitation was 28.2 mm, and so on.

*Properties evaluated:* the mechanical and physical properties, the surface hardness, axial compressive strength, water absorption by total immersion, and water absorption by capillarity were determined. The specimens were dried in an oven at 40±5 °C until the stabilization of the mass and later placed in a desiccator until the tests were carried out. The determination of surface hardness consisted of the

application of a load of 500 N on a sphere of diameter 10±0.5 mm placed in contact with one of the surfaces of the cubic plaster specimen (with dimensions of 50x50x50 mm) [13]. The test was carried out on the underside of the mold and on two other opposite sides of each specimen. After the test, measurements were made of the impression depth of the metallic sphere on the surface of the specimens with the aid of a digital caliper. Thus, the surface hardness,  $D$  (N/mm<sup>2</sup>), value was determined by:

$$D = \frac{F}{\pi \cdot \phi \cdot t} \quad (D)$$

in which,  $F$  is the load (N),  $\phi$  is the sphere diameter (mm), and  $t$  is the average depth (mm). The compressive strength tests were performed in a universal testing machine [14]. The generated data were recorded using a software (Tesc Emic, Intermetric). The value of the compressive strength,  $R$  (MPa), was obtained by:

$$R = \frac{P}{S} \quad (E)$$

in which,  $P$  is the load that produced the rupture of the specimen (N), and  $S$  is the cross-sectional area of load

application (mm<sup>2</sup>). As for the determination of absorption by total immersion [15], the specimens were placed in a container with water at room temperature for 120 min, avoiding touching the bottom of the container and its upper face to remain with a water depth of 5±1 cm. After the period of contact with water, the specimens were removed from the container and superficially dried with a damp cloth. Subsequently, they were weighed, obtaining the wet mass. The water absorption, A (%), of each specimen was determined through:

$$A = \frac{m_2 - m_1}{m_1} \cdot 100 \quad (\text{F})$$

in which,  $m_2$  is the wet mass obtained after immersion of the specimens (g), and  $m_1$  is the initial dry mass after removal from the desiccator (g). To determine the capillarity coefficient, the capillary absorption test was performed [16]. At the beginning of the test, the specimens were weighed and placed in a container with a water depth of 5±2 mm. A mesh supported at a distance of 30 mm from the bottom was used. After contact with water, the specimens were weighed at 5, 30, 60, 120, 240, 360, and 1440 min. The standard determines that during weighing, the net absorption of the specimens is observed. If it is less than 0.001 kg/m<sup>2</sup>, the measurement must be interrupted and the material classified as 'resistant against absorption'. If liquid water is visible on the upper surface of the specimen, the time must be observed and the measurement must be terminated, as the capillary rise will have ended. The amount of water absorbed per surface unit,  $\Delta m_t$  (kg/m<sup>2</sup>), was determined by:

$$\Delta m_t = \frac{m_t - m_1}{A} \quad (\text{G})$$

in which,  $m_t$  is the wet mass of the specimen in the time interval (kg),  $m_1$  is the initial dry mass (kg), and A is the area of the specimen surface (m<sup>2</sup>). Subsequently, the graphs of  $\Delta m_t$  were plotted as a function of the square root of time (s). The behavior of water absorption by capillarity of the materials was classified as type A because the graph of  $\Delta m_t \times$  square root of time showed a linear behavior. Thereby, to determine the capillarity coefficient, the last point of the graph was used, through the equation:

$$A_w = \frac{\Delta m'_{t_f} - \Delta m'_0}{\sqrt{t_f}} \quad (\text{H})$$

in which,  $A_w$  is the capillarity or water absorption coefficient (kg.m<sup>-2</sup>.s<sup>-0.5</sup>),  $\Delta m'_{t_f}$  is the mass gain per surface area in  $t_f$  time (kg/m<sup>2</sup>),  $\Delta m'_0$  is the mass gain per surface area at  $t_0$  time (kg/m<sup>2</sup>), and  $t_f$  is the test duration (s). The analysis of surface hardness, axial compressive strength, and absorption by total immersion took place in cubic specimens (50x50x50 mm), whereas the evaluation of capillary absorption was carried out in prismatic specimens (40x40x160 mm). In these cases, the tests were carried out at 'zero' age (before aging) and after 30, 60, 90, 120, and 150 days of aging, to assess whether the water-repellent action was influenced by the weather to which the specimens

were exposed. The specimens used in the determination of the properties were randomly obtained between the groups (GR, GH2, and GH4), with three specimens being drawn for each test, at each age. For statistical treatment, the Duncan test was applied to compare means. In addition to the tests already listed, an evaluation of the micromorphology was carried out by scanning electron microscopy (SEM) and a semiquantitative analysis of the chemical distribution by energy dispersive spectroscopy (EDS) mapping. Samples extracted from reference specimens (GR) at age zero and with the addition of water repellent (GH4) at age zero and after 150 days of natural aging were evaluated. The procedure was taken with a scanning electron microscope (Vega 3XM, Tescan) at an accelerating voltage of 20 kV, equipped with a secondary electrons detector. The specimen was mounted on a metal stub using a sticky carbon strip that increased conductivity. A gold coating was additionally applied for even more conductivity. The micrographs were performed at a magnification of 3000 times in a low vacuum. The analysis of elements present in sample particles was performed by an energy dispersive spectrometer associated with the equipment. The samples used were extracted in a region close to the surface, since previous analysis, referring to another stage of the research, indicated that the water-repellent is mostly found in the region close to the specimen surface. Fig. 2 shows the sampling point on the surface of the specimen containing the water-repellent. For each age, 36 specimens were molded: 9 for the surface hardness, 9 for axial compressive strength, 9 for absorption by total immersion, and 9 for absorption by capillarity. In total, 216 specimens were tested.



Figure 2: Image of a specimen with the GH4 treatment indicating the region from which the surface sample was extracted.

## RESULTS AND DISCUSSION

**Materials characterization:** the results of the characterization of the beta plaster can be seen in Table III. Casting plasters must have at least 90% of material passing through the sieve with an opening of 0.29 mm [17]. Thus, the analyzed material met this requirement. The specific mass value is influenced by the crystal arrangement and the crystalline structure in the plaster mass, which depend on the conditions of plaster calcination and hemihydrate production [18], which may explain variations in relation to the standard requirement. As for the contents of free and crystallization water, both had values within the allowed by the standard. Free water can be removed when the material is heated and a higher percentage of free water can be linked to exposure to humid environments or improper storage of the material. The crystallization water content demonstrated the condition of calcination of the plaster, showing a relationship with the composition of the plaster, varying between gypsum, hemihydrate, and anhydrite; contents above 6.2% may indicate the presence of uncalcined material and supercalcined under 4.2% [18].

Fig. 3 shows the experimental X-ray powder diffractogram obtained for the beta plaster sample. The experimental XRD pattern was compared with the reference pattern ICSD 79530, corresponding to bassanite, a calcium sulfate hemihydrate ( $\beta$ -CaSO<sub>4</sub>·1/2H<sub>2</sub>O). The peak positions

Table III - Characterization of beta plaster.

Property	Measured value	Normative value*
Particle size <0.29 mm <sup>a</sup> (%)	97.5±0.7	≥90
Bulk density <sup>a</sup> (kg/m <sup>3</sup> )	550±1	≥600
Free water <sup>b</sup> (%)	1.00±0.03	≤1.3
Crystallization water <sup>b</sup> (%)	4.6±0.5	4.2 to 6.2

\*: NBR 13207 standard [17]; test method: <sup>a</sup>: NBR 12127 [9]; <sup>b</sup>: NBR 12130 [10].

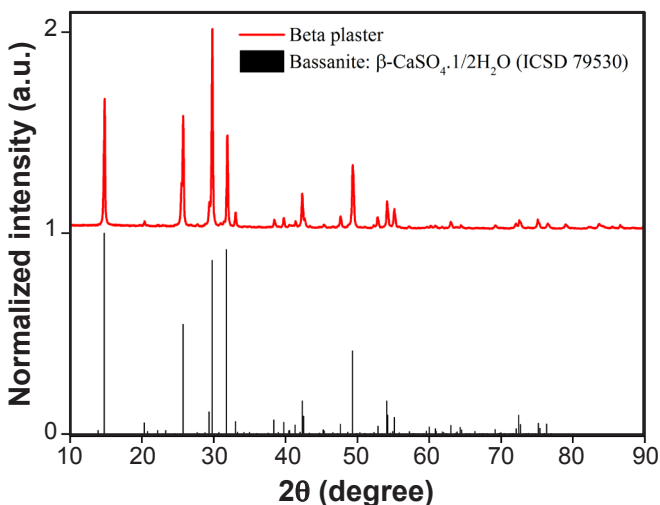


Figure 3: Experimental X-ray powder diffractogram of beta plaster sample and the reference pattern ICSD 79530.

and intensities were corresponding, demonstrating the compatibility of crystalline structures. The highest peaks were found at  $2\theta = 14.77^\circ, 25.70^\circ, 29.76^\circ, 31.78^\circ,$  and  $49.29^\circ$  corresponding to the planes (200), (020), (400), (204), and (42 $\bar{4}$ ), respectively. The material analyzed corresponded mostly to calcium sulfate hemihydrate, which belongs to the monoclinic crystal system having the space group I121. The crystallographic parameters were:  $a=11.9845 \text{ \AA}, b=6.9292 \text{ \AA}, c=12.7505 \text{ \AA}, \alpha=\beta=\gamma=90^\circ,$  volume= $1058.84 \text{ \AA}^3,$  and density= $2.76 \text{ g/cm}^3$ .

Fig. 4a shows the plaster absorption spectrum in the infrared region obtained by FTIR. The presence of its functional groups was identified, with bands at 1620, 1686, 3244, 3406, and 3545 cm<sup>-1</sup> referring to the group -OH, attributed to the water molecules found in the structure of calcium sulfate dihydrate. The sulfate groups (SO<sub>4</sub><sup>2-</sup>) present in the plaster were identified at 602, 667, 1130, and 2234 cm<sup>-1</sup> bands [19, 20]. The absorption spectrum in the infrared

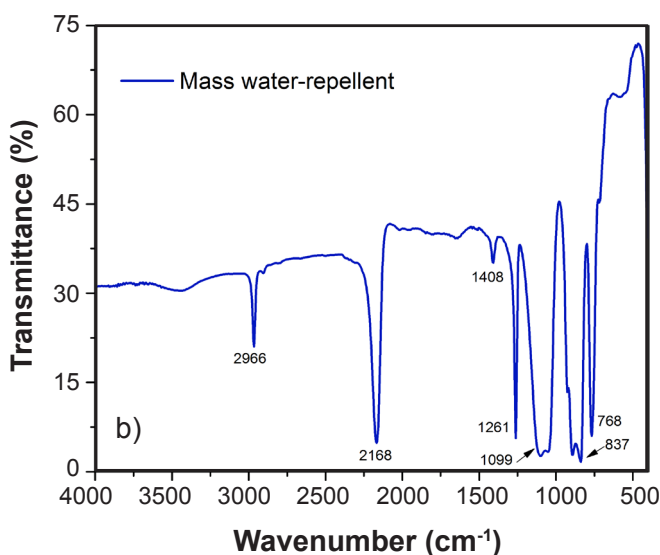
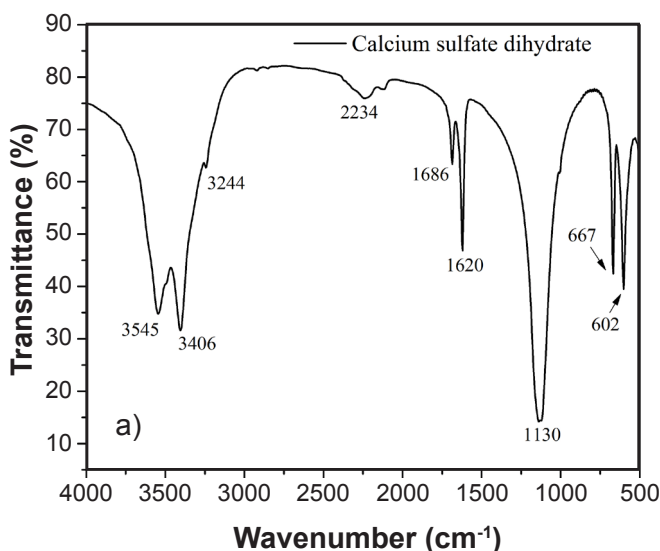


Figure 4: FTIR spectra of calcium sulfate dihydrate (a) and water repellent (b).

region of the mass water-repellent obtained by FTIR is shown in Fig. 4b. The band located at  $2966\text{ cm}^{-1}$  was due to the elongation vibration of  $-\text{CH}_3$ , indicating that the water-repellent in question had a silicone structure containing the methyl functional group [21]. At  $2168\text{ cm}^{-1}$  there was an intense band caused by the presence of the Si-H bond. At  $768$ ,  $1261$ , and  $1408\text{ cm}^{-1}$ , asymmetric vibration in the plane of  $\text{CH}_3$  and elongation vibration of Si-C bond, symmetric strain vibration of Si- $\text{CH}_3$  or Si- $(\text{CH}_3)_2$  bonds, and bending vibration of CH on Si- $\text{CH}_3$  bond, respectively, occurred [22]. The peak present at  $837\text{ cm}^{-1}$  was related to Si-H bond bending vibration. The characteristic Si-O absorption band appeared around  $1099\text{ cm}^{-1}$  [21, 23]. The identified bands indicated that the mass water repellent contained silane/siloxane.

**Mechanical and physical properties. Surface hardness:** Fig. 5a shows the surface hardness values for the specimens produced. It was observed that the samples remained without major variations throughout aging. After 150 days of aging, the surface hardness of the specimens was  $25.13$ ,  $24.00$ , and  $24.45\text{ N/mm}^2$  for GR, GH2, and GH4, respectively. The initial hypothesis was that there would be a decrease in surface hardness over time in the reference specimens (GR), since the rains that occurred during the period could lead to wear of the material, negatively interfering with the mechanical properties. However, it was noticed that the wear was more accentuated only on the upper face, where rain and solar radiation hit more intensely and directly, and that it was not evaluated in the hardness test, since the lower molding surface was evaluated, and on two other two opposite faces [15]. In relation to the specimens containing the water-repellent, even on the upper face, the wear was noticeably lower compared to the GR. For Silva et al. [12], who evaluated the effects caused by the addition of commercial water-repellents on the physical and mechanical properties of casting plaster, the addition of a siloxane-based water-repellent led to a decrease in hardness, unlike what happened with the treatments GH2 and GH4, in the present research. There was a significant variation between age zero and after 150 days of aging for the GH4 treatment. On the other hand, there was no significant variation between age zero and after 150 days in the reference specimens (GR) and GH2 type. According to standard recommendations, a

minimum value of  $20\text{ N/mm}^2$  is established for specimens molded in normal consistency [11]. The water/plaster ratio used was  $0.7$ , certainly higher than necessary to obtain a normal consistency. However, even with the water/plaster ratio used, after 150 days of natural aging, all specimens continued to reach values above  $20\text{ N/mm}^2$ .

**Axial compressive strength:** Fig. 5b shows the axial compressive strength values after natural aging over 150 days of exposure. The exposed specimens did not show a linear behavior over the 150 days, thus that there was a gain and subsequent loss of materials strength that were subjected to different treatments. In the reference specimens (GR), maximum resistance was reached at 120 days. In the GH2 and GH4 treatments, there was an increase in resistance up to 90 days of natural aging, followed by a decrease up to 150 days of aging, which demonstrated a non-linear behavior over time. The causes of the variations in the plaster properties that occurred during the aging process were not yet consolidated, which means that there are still some uncertainties about the mechanisms involved. In Table II, it can be seen that at 90 days of aging, there was the highest precipitation in relation to the entire period in which the specimens were exposed. Thus, the greater volume of rains may have led to a decrease in precipitation resistance in the GR-type specimens (without water-repellent) in this period (Fig. 5b). From the statistics, there was no difference between the resistance obtained at 150 days of aging in relation to the zero age in the GR, GH2 and GH4 treatments. It is also noticed that there was no difference between the resistance obtained at 150 days of aging in relation to the zero age in the GR, GH2, and GH4 treatments. The standard recommends a minimum compressive strength of  $8.4\text{ MPa}$  for a building plaster produced with the water/plaster ratio at normal consistency [24]. Thus, despite the water/plaster ratio being  $0.7$ , which leads to a more porous microstructure due to the evaporation of water that does not participate in the hydration process, it was possible to obtain strengths greater than  $8.4\text{ MPa}$  even after exposure to inclement weather.

**Absorption by total immersion:** total immersion absorption values over natural aging are shown in Fig. 6a. It was noted that the reference treatment maintained an almost constant absorption over time, however, the addition of the mass water-repellent significantly reduced water

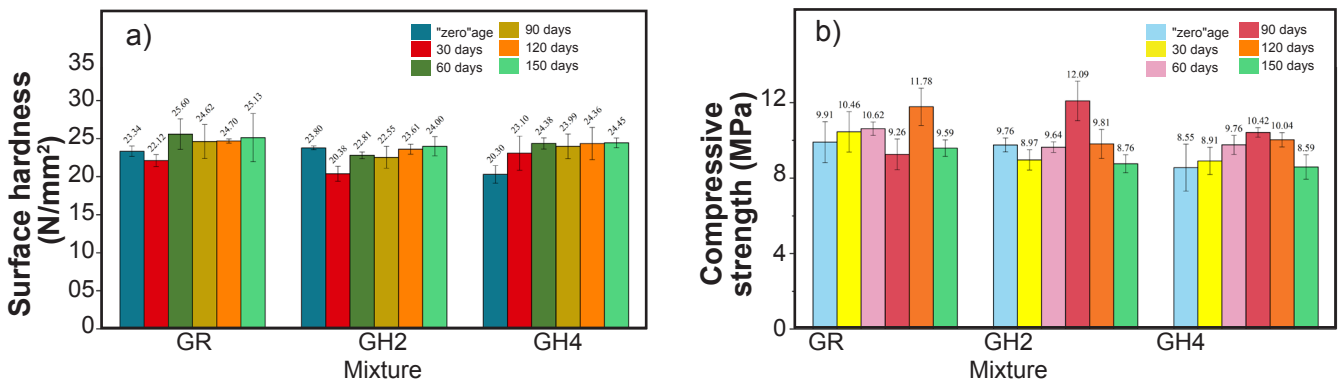


Figure 5: Hardness (a) and compressive strength (b) of plaster samples during natural aging.

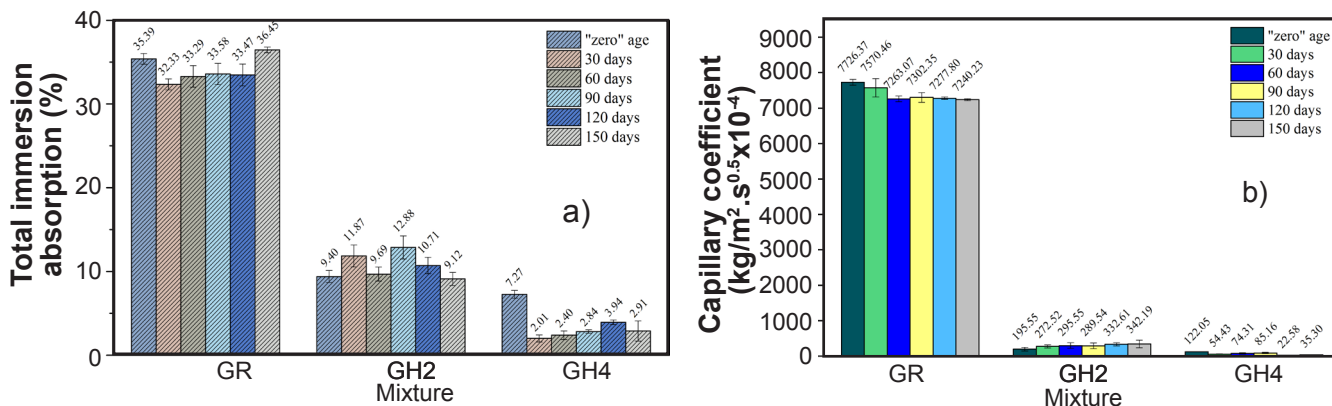


Figure 6: Total immersion absorption (a) and capillary coefficient (b) during natural aging.

absorption. In the GH2 treatment, there was a reduction in absorption to below 15%, with small variations throughout aging. Regarding the GH4 treatment, there was a reduction in absorption at 30 days, compared to the zero age, to values below 5%. This is because when added to a plaster slurry to form silicone resins *in situ*, siloxane can take a long time to cure. The siloxane forms a reactive silanol intermediate to produce polymethylsilicic acid, which cross-links to form the silicone resin. This reaction occurs slowly, and continues after the hardening of the plaster, requiring days for water resistance to develop [25], which justifies the decrease in absorption in the following ages. The absorption percentage found after 150 days of aging was 2.91% for the addition of 0.4% of water-repellent (GH4). This value was similar to that obtained by Li *et al.* [22], when evaluating the water resistance of an organosilicon water-repellent, in a content of 1% in relation to the plaster mass after 60 min of testing, with an absorption of 2.73%. As for standard compliance, only the GH4 treatment complied with the EN 12859 [26] regarding the absorption that classifies plaster blocks as type H2 (water absorption  $\leq 5\%$ ), as well as the NBR 16494 [27]. According to the classification of the EN 520 [28], both the GH4 and the GH2 treatment met the established value for type H2 plasterboard (water absorption  $\leq 10\%$ ).

**Capillary absorption:** Fig. 6b shows the capillary coefficient obtained in each treatment. It was noted that the treatments with the best results were GH2 and GH4. The GH2 treatment obtained an increasing capillarity coefficient over time. From this behavior, it was hypothesized that this result was correlated with the concentration of the water-repellent on the specimen surface and that the wear of this surface would gradually remove the water-repellent. This is because the product must be well distributed throughout the plaster matrix to obtain a good hydrophobic result. However, the specimens with a greater amount of water-repellent maintained a low absorption by capillarity. This can be explained by the presence of the water-repellent in the matrix of the specimen, which forms a film that surrounds the crystals. The water-repellent is formed by a polar part (Si-O) and a non-polar organic part (CH<sub>3</sub>), which allows the polar part of the water-repellent to be attracted to the surface of the dihydrate, in order that the part of the molecule is

oriented towards the outside, which forms a non-polar barrier and makes it difficult for the plaster to absorb water.

The period between when the specimens were placed in the field and when they were collected at 90 days was the wettest, among the period of total exposure. The rainfall occurrence, temperature variations, and other environmental factors led to wear on the surface of the specimens, which were higher in those with 0.2% (GH2) of water-repellent, unlike those with 0.4% (GH4). Surface wear (Figs. 7 to 9) facilitates water absorption. However, even with this reduction in barrier efficiency, the capillary coefficient ( $A_w$ ) was considerably lower than that of the reference specimen (GR). Thus, the GH4 treatment proved to be the most efficient over aging when compared to the other treatments. In Fig. 9 it is noticed that there was the appearance of numerous superficial pores due to the dissolution of the plaster, which was 2 g/L [1]. As the amount of water-repellent incorporated into the plaster increased, there was a reduction in the dissolution and, consequently, a smaller amount of pores on the surface of the material, as shown in Figs. 8 and 9. Another characteristic observed was the change in the color of the specimens after exposure to the weather, which showed a yellowing of the surface of the material caused by the incidence of solar radiation. Bonds between silicon and oxygen present in the water-repellent present high binding energy, which resulted in greater resistance to photooxidation. This represented a possible explanation for why the change in color was smaller as the amount of water-repellent incorporated was increased.

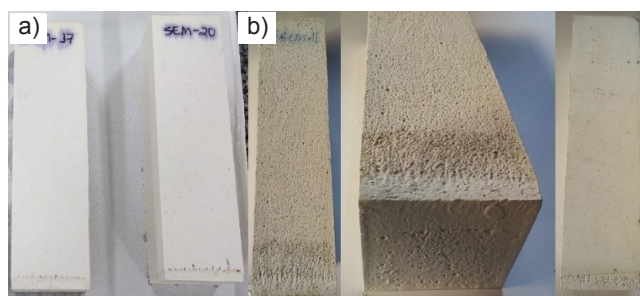


Figure 7: Images of reference specimens (GR) at zero age (a) and after 150 days of aging (b). In addition to the color change, there was also greater surface porosity.

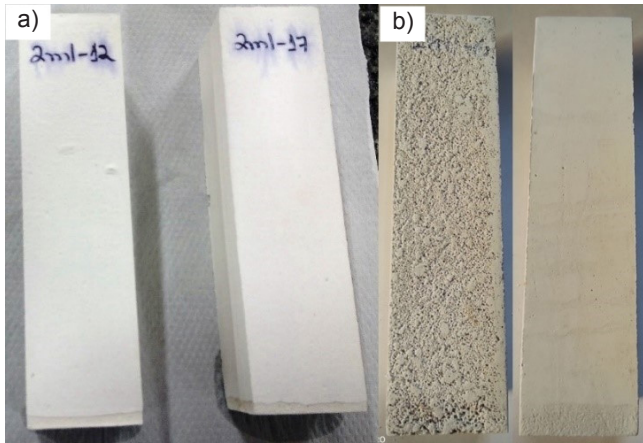


Figure 8: Images of GH2 specimens at zero age (a) and after 150 days of aging (b). The most degraded face was the one turned up, exposed to weathering. The lateral faces and that in contact with the support were better preserved.

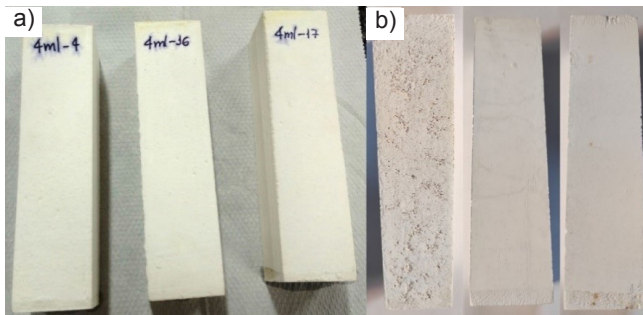


Figure 9: Images of GH4 specimens at zero age (a) and after 150 days of aging (b). The degradation of the face more exposed to weathering was lower in the GH4 mixture, compared to the GH2 and GR specimens.

The capillarity coefficient obtained with the GH2 treatment at 150 days was  $342.2 \times 10^{-4} \text{ kg}/(\text{m}^2 \cdot \text{s}^{0.5})$ . This result corroborated that obtained by Santos et al. [29], who used 0.2% of silicone-based water-repellent. However, in the reported research, the specimens were not exposed to natural aging. Regarding the GH4 treatment, the capillarity coefficient was lower than the one observed by Santos et al. [29], who obtained a minimum coefficient of  $1.70 \times 10^{-2} \text{ kg}/(\text{m}^2 \cdot \text{s}^{0.5})$  for a dosage of 0.4% siloxane-based water-repellent. In a statistical analysis, there was a variation in the capillarity coefficient values during natural aging. Based on the classification of EN 52617 [30] at 150 days, the GH4 treatment was referred to as ‘almost impermeable’ because it resulted in an absorption coefficient lower than  $83.3 \times 10^{-4} \text{ kg}/(\text{m}^2 \cdot \text{s}^{0.5})$ . The other treatment was referred to as ‘quick suction’ material.

*Scanning electron microscopy (SEM) and energy dispersive spectroscopy (EDS) mapping:* Fig. 10a shows an SEM micrograph of calcium sulfate dihydrate, without the addition of water-repellent, before natural aging. The presence of elongated and bundled dihydrate crystals was identified, as well as smaller crystals and the presence of plaques. Fig. 10b shows the elements identified through

energy dispersive spectroscopy (EDS). The presence of oxygen (O), calcium (Ca), and sulfur (S) was noted, corresponding to the composition of calcium sulfate dihydrate, whose chemical mapping is present in Fig. 11.

Fig. 12 shows micrographs of the sample submitted to the GH4 treatment. It was observed that the crystal morphology was different if compared to the reference plaster (GH), due to the presence of the water-repellent in the matrix. In addition,

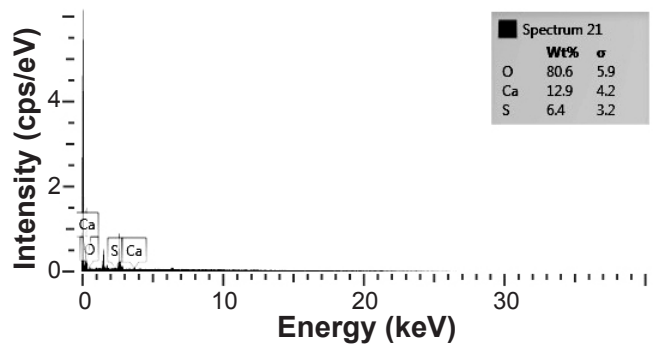
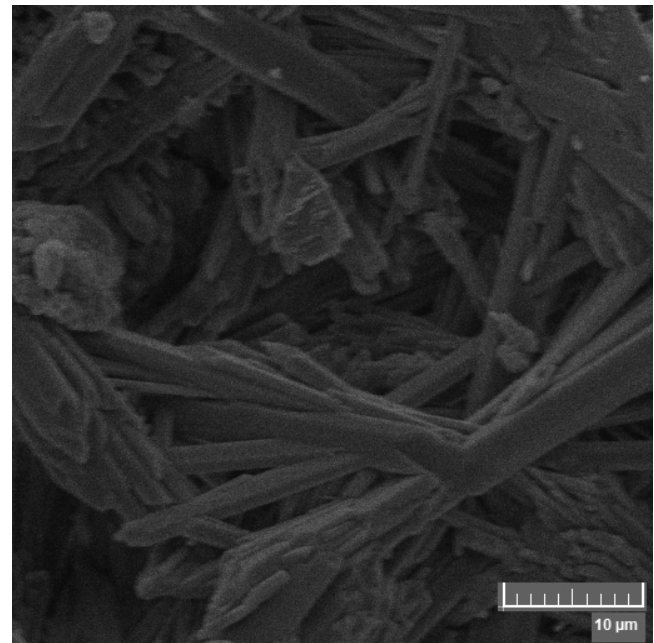


Figure 10: SEM micrograph (a) and EDS spectrum (b) of plaster, calcium sulfate dihydrate, without the addition of water-repellent (GH) before natural aging.

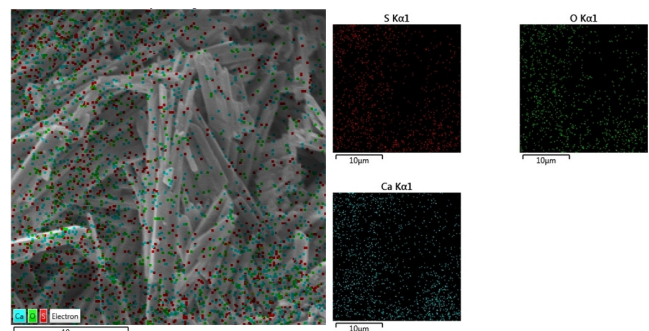


Figure 11: EDS chemical mapping of the plaster without the addition of water-repellent.

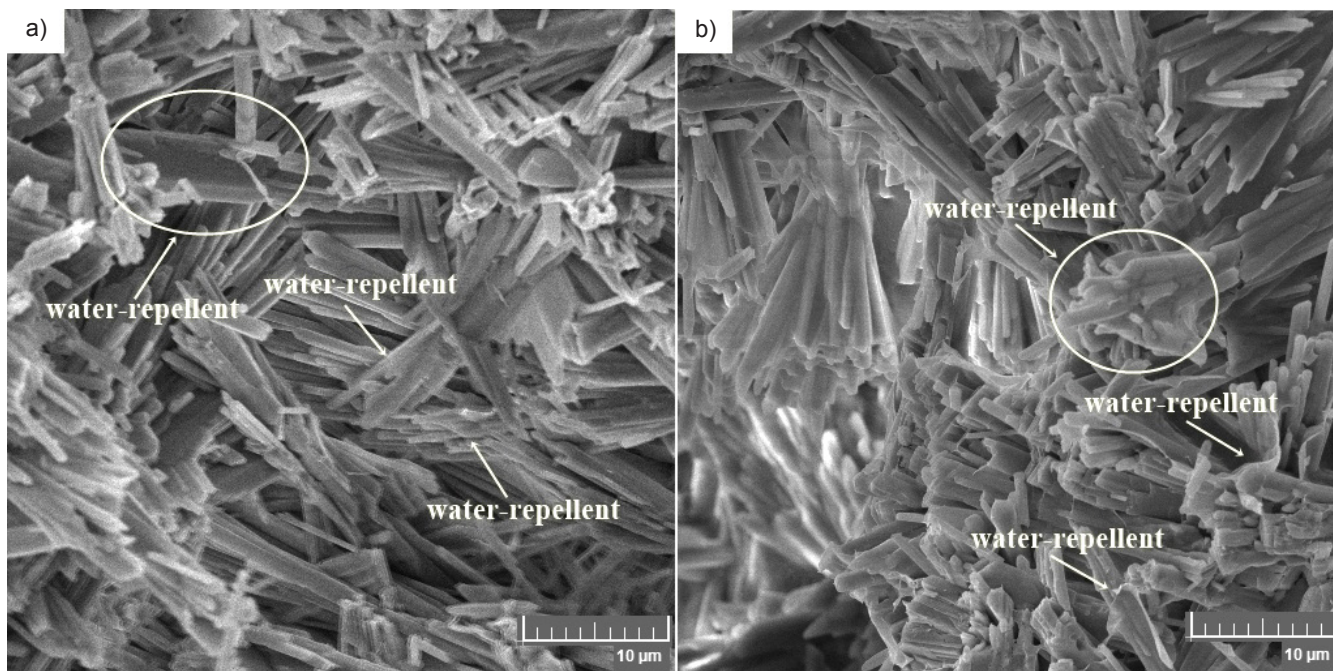


Figure 12: SEM micrographs of the specimen submitted to the GH4 treatment before, zero age (a), and after 150 days of aging (b). It is possible to visualize the presence of water-repellent even after the aging process.

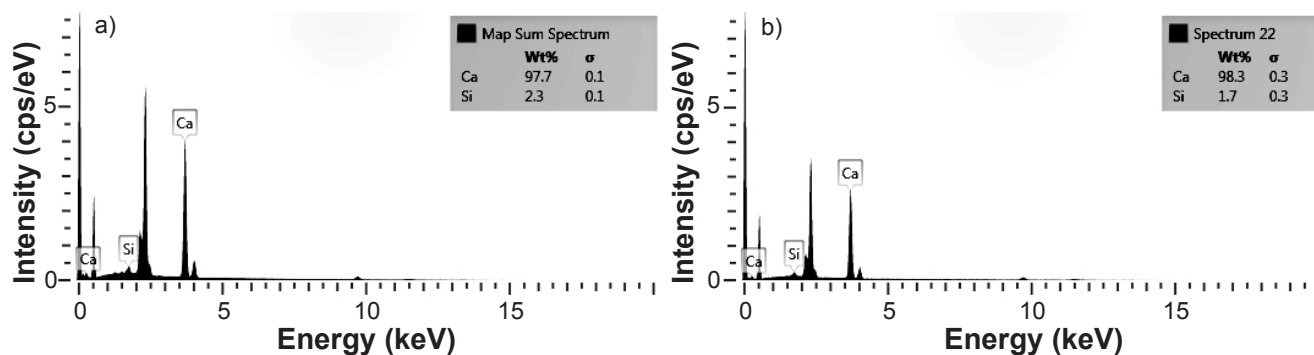


Figure 13: EDS spectra of the specimen submitted to the GH4 treatment at zero age (a) and after 150 days of aging (b).

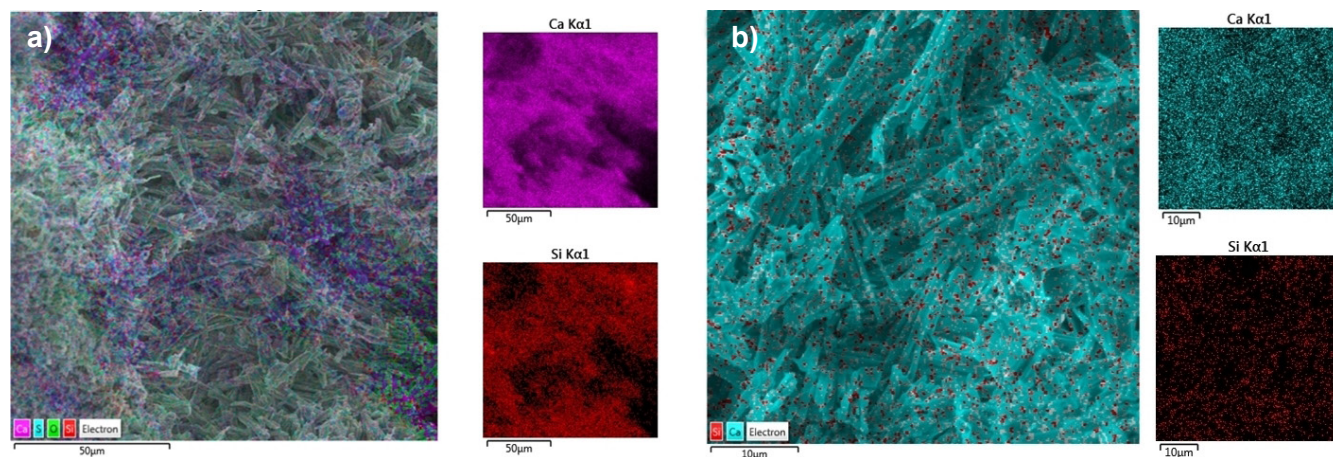


Figure 14: EDS chemical mapping of the specimen submitted to the GH4 treatment at zero age (a) and after 150 days of aging (b).

there were crystal tufts wrapped in the water-repellent. After 150 days of aging (Fig. 12b), the water-repellent was still present in the matrix, identified by the presence of crystals

engulfed by the material, and by a film that was visible at various points in the micrograph. The water-repellent agent adsorbed on the surface of the crystals surrounding

them, thereby impeding hindering the migration of water between the crystals. Fig. 13 shows the EDS spectra and the respective chemical composition for the sample under the GH4 treatment. The presence of mass water-repellent in the matrix was confirmed, which corresponded to silicon (Si) of the silane/siloxane composition, which was present in small contents, due low water-repellent/plaster ratio. EDS analysis is a semi-quantitative technique complementary to SEM. Therefore, the percentages found should not be taken as absolute values for the entire specimen. This analysis indicated that it was possible to identify the presence of water-repellent even after aging and with the use of small additive content (about 0.4% in relation to the plaster mass). The EDS chemical mapping (Fig. 14) shows the distribution of elements in the matrix for the sample submitted to the GH4 treatment. The water-repellent was homogeneously distributed throughout the evaluated matrix.

## CONCLUSIONS

It was concluded that: i) at 150 days of natural aging, the evaluated mechanical properties (surface hardness and axial compressive strength) did not undergo major changes, with values still meeting the standard recommendations; ii) when using 0.4% of mass water-repellent (GH4 treatment), there was a reduction in absorption by total immersion to values below 5%, even after aging; iii) there was a considerable reduction in the capillary coefficient with the use of mass water-repellent, whose effect remained throughout natural aging at a value of 0.4%; iv) the mechanical and absorption properties did not undergo major changes when compared with the results of the tests at the 'zero' age, even after exposure to the natural aging, indicating the effectiveness of adding the mass water-repellent; and e) for the microstructure, it was still possible to identify the presence of water-repellent in the matrix after natural aging. This study showed that the use of water-repellent did not interfere with the mechanical properties, even after exposure for 150 days. However, the waterproofing capacity occurred only in the blocks with water-repellent. Furthermore, wear was visually observed only in a thin superficial layer. In addition, it was noticed that the surface wear was higher in the specimens without water-repellent. Thus, the study indicated that plaster is a promising material for the production of sealing blocks to be used in regions with a climate similar to that of the research site. Studies of aging for longer exposure periods may provide complementary results to this research.

## REFERENCES

[1] M. Garg, A. Pundir, R. Singh, *Mater. Struct.* **49**, 8 (2016) 3253.  
 [2] H.J.B. Lima Filho, "Tratamento dos resíduos de gesso da construção e da demolição - RCD para a produção de gesso beta reciclado", M.Sc. Diss., UFPE, Recife (2010).  
 [3] J. Bochen, *Constr. Build. Mater.* **79**, 15 (2015) 192.  
 [4] C. Chai, J. Brito, A. Silva, P.L. Gaspar, *Rev. Eng. Civ.*

**41** (2011) 51.  
 [5] V. Fassina, M. Favaro, A. Naccari, M. Pigo, *J. Cult. Herit.* **3**, 1 (2002) 45.  
 [6] G. Camarini, J.A. De Milito, *Constr. Build. Mater.* **25** (2011) 4121.  
 [7] N. Belayachi, D. Hoxha, M. Slaimia, *Constr. Build. Mater.* **125**, 30 (2016) 912.  
 [8] S.D.S. Rodrigues, J.G.G. Sousa, A.C. Dantas, L.I.N. Hernández, M.A. Silva, N.C. Olivier, *Rev. Eng. Pesq. Apl.* **6**, 3 (2021) 64.  
 [9] NBR 12127, "Gesso para construção: determinação das propriedades físicas do pó", Ass. Bras. Norm. Técn., Rio Janeiro (2019).  
 [10] NBR 12130, "Gesso para construção: determinação da água livre e de cristalização e teores de óxido de cálcio e anidrita", Ass. Bras. Norm. Técn., Rio Janeiro (1991).  
 [11] NBR 11768, "Aditivos químicos para concreto de cimento Portland, parte 3: ensaios de caracterização", Ass. Bras. Norm. Técn., Rio Janeiro (2019).  
 [12] D.B.P. Silva, J.G.G. Sousa, D.C.E. Ferreira, T.M.C. Rodrigues, in *Proc. Enc. Nac. Tecnol. Amb. Constr.*, ANTAC, Foz Iguaçu (2018).  
 [13] NBR 12129, "Gesso para construção: determinação das propriedades mecânicas", Ass. Bras. Norm. Técn., Rio Janeiro (2019).  
 [14] NBR 12129, "Gesso para construção: determinação das propriedades mecânicas", Ass. Bras. Norm. Técn., Rio Janeiro (1991).  
 [15] NBR 16495, "Bloco de gesso para vedação vertical: método de ensaio", Ass. Bras. Norm. Técn., Rio Janeiro (2016).  
 [16] C1794-15, "Standard test methods for determination of the water absorption coefficient by partial immersion", Am. Soc. Test. Mater., USA (2015).  
 [17] NBR 13207, "Gesso para construção civil: requisitos", Ass. Bras. Norm. Técn., Rio Janeiro (2017).  
 [18] F.C. Ferreira, J.G.G. Sousa, A.M.P. Carneiro, *Amb. Constr.* **19**, 4 (2019) 207.  
 [19] P.S.R. Prasad, V.K. Chaitanya, K.S. Prasad, D.N. Rao, *Am. Miner.* **90**, 4 (2005) 672.  
 [20] A.A. Barbosa, A.V. Ferraz, G.A. Santos, *Cerâmica* **60**, 356 (2014) 501.  
 [21] W. Zhang, X. Zou, X. Liu, Z. Liang, Z. Ge, Y. Luo, *Prog. Org. Coa.* **139** (2020) 105.  
 [22] Z. Li, K. Xu, J. Peng, J. Whang, J. Zhang, *Case Stud. Constr. Mater.* **14** (2021) 1.  
 [23] D.L. Pavia, G.M. Lampman, G.S. Kriz, J.R. Vyvyan, "Introdução à espectroscopia", CENGAGE Learn. (2013).  
 [24] NBR 13207, "Gesso para construção civil: requisitos", Ass. Bras. Norm. Técn., Rio Janeiro (1994).  
 [25] X. Wang, Q. Liu, P. Reed, Q. Yu, "Siloxane polymerization in wallboard", United States Patent, 8501074B2 (2010).  
 [26] EN 12859, "Gypsum blocks: definitions, requirements and test methods", Brit. Stand. (2011).  
 [27] NBR 16494, "Bloco de gesso para vedação vertical: requisitos", Ass. Bras. Norm. Técn., Rio Janeiro (2017).

[28] EN 520, “Europäische normung für gipsplatten”, Deut. Inst. Norm., Germany (2009).

[29] A.N. Santos, N.M.M. Ramos, J.F. Maia, in Proc. 59<sup>th</sup> Congr. Bras. Concr., IBRACON, Bento Gonçalves (2017).

[30] DIN 52617, “Determination of the water absorption coefficient of construction materials”, Deut. Inst. Norm. (1987).

(*Rec.* 18/10/2021, *Rev.* 08/04/2022, 19/06/2022, *Ac.* 23/06/2022)

